



UvA-DARE (Digital Academic Repository)

Translating lipid-driven inflammation in atherosclerosis

van der Valk, F.M.

Publication date

2016

Document Version

Final published version

[Link to publication](#)

Citation for published version (APA):

van der Valk, F. M. (2016). *Translating lipid-driven inflammation in atherosclerosis*. [Thesis, fully internal, Universiteit van Amsterdam].

General rights

It is not permitted to download or to forward/distribute the text or part of it without the consent of the author(s) and/or copyright holder(s), other than for strictly personal, individual use, unless the work is under an open content license (like Creative Commons).

Disclaimer/Complaints regulations

If you believe that digital publication of certain material infringes any of your rights or (privacy) interests, please let the Library know, stating your reasons. In case of a legitimate complaint, the Library will make the material inaccessible and/or remove it from the website. Please Ask the Library: <https://uba.uva.nl/en/contact>, or a letter to: Library of the University of Amsterdam, Secretariat, Singel 425, 1012 WP Amsterdam, The Netherlands. You will be contacted as soon as possible.

CHAPTER 9

PREDNISOLONE-CONTAINING LIPOSOMES ACCUMULATE IN HUMAN ATHEROSCLEROTIC MACROPHAGES UPON INTRAVENOUS ADMINISTRATION

Van der Valk FM*, van Wijk DF*, Lobatto M, Verberne HJ, Storm G, Willems MCM, Legemate DA, Nederveen AJ, Calcagno C, Venkatesh M, Ramachandran S, Paridaans MPM, Otten MJ, Dallinga GM, Fayad ZA, Nieuwdorp M, Schulte DM, Metselaar JM, Mulder WJM, Stroes ESG.

* Authors contributed equally

Nanomedicine. 2015;11:1039-46

ABSTRACT

Rationale: Drug delivery to atherosclerotic plaques via liposomal nanoparticles may improve therapeutic agents' risk-benefit ratios. Our paper details the first clinical studies of a liposomal nanoparticle encapsulating prednisolone (LN-PLP) in atherosclerosis.

Methods and Results: First, PLP's liposomal encapsulation improved its pharmacokinetic profile in humans (n=13) as attested by an increased plasma half-life of 63 hours (LN-PLP 1.5 mg/kg). Second, intravenously infused LN-PLP appeared in 75% of the macrophages isolated from iliofemoral plaques of patients (n=14) referred for vascular surgery in a randomized, placebo-controlled trial. LN-PLP treatment did however not reduce arterial wall permeability or inflammation in patients with atherosclerotic disease (n=30), as assessed by multimodal imaging in a subsequent randomized, placebo-controlled study.

Conclusion: In conclusion, we successfully delivered a long-circulating nanoparticle to atherosclerotic plaque macrophages in patients, whereas prednisolone accumulation in atherosclerotic lesions had no anti-inflammatory effect. Nonetheless, the present study provides guidance for development and imaging-assisted evaluation of future nanomedicine in atherosclerosis.

INTRODUCTION

Because inflammation plays a pivotal role in atherosclerotic plaque development¹, novel anti-inflammatory strategies² are expected to complement and improve existing therapeutic regimens. Delivering drugs via nanocarriers may reduce atherosclerotic plaque inflammation by enhancing drug accumulation at target sites, without compromising immunity³. Though several liposomally formulated anticancer drugs have already been approved for clinical use⁴, nanomedicine remains unexplored in patients with cardiovascular disease. Theoretically, an inflamed atherosclerotic plaque, characterized by endothelial dysfunction and a highly permeable microvasculature, could be an excellent target for nanomedicinal delivery⁵.

Of the numerous clinically-applied anti-inflammatory compounds, glucocorticoids (GC) are the most widely used and have potent anti-inflammatory effects⁶. However, systemic GC treatment has not been used in patients with cardiovascular disease because long-term GC use has pro-atherogenic effects, including dyslipidemia, glucose intolerance and hypertension⁷. In contrast, locally administering GC via drug-eluting stents has been shown to reduce neo-intimal formation and arterial wall inflammation in an experimental model⁸. These results suggest a liposomal GC formulation may minimize systemic adverse effects while improving local anti-inflammatory efficacy. In support of this idea, we previously reported markedly reduced arterial wall inflammation following intravenous administration of liposomal prednisolone in an atherosclerotic rabbit model⁹.

Here we evaluate the clinical applicability of a long-circulating liposomal nanoparticle encapsulating prednisolone phosphate (LN-PLP) in patients with atherosclerosis. First, we determined liposomal prednisolone's pharmacokinetic profile in humans and assessed delivery to plaque macrophages isolated from iliofemoral plaques of patients referred for vascular surgery. Subsequently, we used noninvasive multimodal imaging to measure the anti-inflammatory efficacy of LN-PLP in patients with atherosclerosis.

METHODS

Study participants

All participants provided written informed consent. The clinical trials were approved by the local institutional review board and conducted according to the principles of the International Conference on Harmonisation–Good Clinical Practice guidelines (Clinicaltrials.gov registration NCT01039103, NCT01647685, NCT01601106).

Liposomal prednisolone

The liposomal nanoparticles (LN) were composed of a hydrophilic core encapsulating prednisolone phosphate (PLP), surrounded by a lipid bilayer of phospholipids and cholesterol, which was coated with polyethylene glycol (PEG). See supplementary methods for LN-PLP formulation.

Pharmacokinetic profile of LN-PLP in humans

We conducted a single-dose escalation study, using 13 subjects, to determine the pharmacokinetic performance of LN-PLP after a single intravenous (i.v.) dose of 0.375 mg/kg (n=3), 0.75 mg/kg (n=3) or 1.5 mg/kg (n=7) LN-PLP in a 2.5 hour time frame. Serum concentrations of PL and its pro-drug PLP were measured on days 1, 3, 7 and weekly up to 12 weeks using high-performance liquid chromatography. Safety evaluation after LN-PLP administration included documenting adverse events, checking vital signs and conducting safety laboratory tests.

LN-PLP delivery in patients with iliofemoral atherosclerosis

To study LN-PLP's delivery, we performed a randomized, placebo-controlled, double-blind trial in 14 patients with iliofemoral atherosclerotic plaques who were scheduled for endarterectomy. After 1:1 randomization, patients received either 1.5 mg/kg LN-PLP (n=7) or saline (n=7) via an antecubital vein on days 0 and 7, followed by vascular surgery on day 10. The dosing regimen for LN-PLP was based on a preclinical study in rabbits⁹ and adjusted according to the drug-dose conversion from rabbit to human¹⁰. Plaque tissue macrophages were isolated to evaluate the presence of LN-PLP (see Supplementary methods). Cells were spotted on a glass slide using a cytospin centrifuge, fixed with 0.4% paraformaldehyde (30min), permeabilized with 0.1% Triton X-100 (10min) and stained overnight. Primary antibodies were mouse anti-human CD68 (Abcam, Cambridge, UK; 1:100) and rabbit anti-human PEG (Epitomics, Burlingame, CA, U.S.A.; 1:100), and secondary antibodies were CyTM3-conjugated donkey anti-mouse and FITC-conjugated donkey anti-rabbit (both Jackson, West Grove, PA, 1:200). Cells were examined with fluorescence microscopy (Leica, DMRA HC Upright). Per patient, at least 4 cell spin slides were used to examine the percentage of DAPI cells positive for CD68 (macrophages) and, DAPI/CD68 cells positive for PEG (LN-PLP). A reader who was blinded for treatment allocation performed these analyses.

Local efficacy in patients with atherosclerosis

Subsequently, we evaluated LN-PLP therapeutic efficacy in a randomized, placebo-controlled, double-blind trial of 30 patients with documented history of atherosclerotic cardiovascular disease (i.e. angina pectoris, myocardial infarction, TIA or stroke). Prospective participants

underwent ^{18}F fluorodeoxyglucose positron emission tomography with computed tomography (^{18}F -FDG PET/CT) to identify patients with marked arterial wall inflammation ($\text{TBR}_{\text{max}} > 2.2$, measured in either the ascending aorta or carotid arteries). Based on this criterion, five (14%) of the 36 subjects screened were not included in the study. After enrolment, patients had dynamic contrast enhanced-magnetic resonance imaging (DCE-MRI) scans of their carotid arteries prior to treatment allocation. One of the remaining 31 patients dropped out due to claustrophobia during baseline MRI acquisition. After 2:1 randomization, patients received either LN-PLP 1.5 mg/kg ($n=20$) or saline ($n=10$) i.v. on days 0 and 7. On day 10, we assessed therapeutic efficacy by DCE-MRI and ^{18}F -FDG PET/CT imaging of both carotid arteries. A blinded, experienced reader analyzed the images at the core laboratory (TMII, Department of Radiology, Mount Sinai). Prior to analysis, the image set was assessed for quality, and standard operating procedures ensured that the same arterial segments, based on specified anatomical locations, would be analyzed by both PET/CT and (DCE)-MRI (see Supplementary methods).

Statistical analysis

Baseline values and distributional characteristics are shown as mean (SD), number (frequency) or median (min-max). Independent samples t-test, Mann-Whitney U test and Chi-square test were used to assess baseline differences between patients and controls. For efficacy analysis, Wilcoxon signed-rank test was used. A two-sided P -value below 0.05 was considered statistically significant. All data were analyzed using Prism version 5.0 (GraphPad software, La Jolla, CA, USA) and SPSS version 19.0 (SPSS Inc., Chicago, IL, USA).

RESULTS

Pharmacokinetic performance of LN-PLP in humans

Prior to investigating delivery and efficacy of LN-PLP in humans, we studied its PK profile in 13 subjects, 8 male and 5 female, with a mean age of 51 ± 10 years (Table 1). LN-PLP had a prolonged circulation half-life ($t_{1/2}$) ranging from 45 to 63 hours. The area-under-the-curve for LN-PLP indicated a dose-dependent relationship (from 856 ± 171 , 1355 ± 352 , to 4135 ± 1489 $\mu\text{g}\cdot\text{h}/\text{mL}$ for 0.375, 0.75 and 1.5 mg/kg LN-PLP, respectively). The peak plasma concentration of free PL was, on average, 0.5% of the total liposomal PLP plasma concentration and remained constant throughout the 28-day experimental period (Figure S1). This constancy indicates negligible encapsulated drug leakage from the liposome into circulation, since direct leakage would accelerate PLP plasma decay and increase the percentage of free PL. Table 1 provides an overview of PK data in humans. LN-PLP was well tolerated, and no serious adverse events occurred. Further, LN-PLP did not adversely affect cardiometabolic parameters, nor did it significantly change liver and/or kidney parameters (Table S1).

TABLE 1. Pharmacokinetic properties of LN-PLP in humans

Clinical characteristics	0.375 mg/kg (n = 3)	0.75 mg/kg (n = 3)	1.5 mg/kg (n = 7)
Age (years)	53 ± 12	44 ± 5	57 ± 12
Gender (male %)	2 (67)	2 (67)	4 (57)
PK parameters			
AUC (0-168h) (µg.ml.h ⁻¹)	856 ± 171	1355 ± 352	4135 ± 1489
t _{1/2} (hr)	45.0 ± 26.0	42.7 ± 12.8	62.5 ± 11.9
CL (L/hr)	0.041 ± 0.011	0.054 ± 0.016	0.031 ± 0.010
PL/PLP ratio	0.55	0.65	0.41

Data are shown as mean ± SD or number (%). AUC indicates area under the concentration curve; t_{1/2}, half-life; CL, plasma clearance; LN-PLP, liposomal prednisolone; PL/PLP ratio, proportion free prednisolone of total liposomal prednisolone phosphate; V_{ss}, volume of distribution at steady state.

Delivery of LN-PLP to plaque macrophages in patients

LN-PLP plaque delivery was evaluated in 14 patients, with a mean age of 70 ± 7 years, who were scheduled for endarterectomy due to symptomatic iliofemoral atherosclerosis. Patients were divided into two groups, one to receive LN-PLP and the other a placebo, with comparable clinical characteristics (Table 2). After surgery on day 10 post-treatment, macrophages were isolated from excised plaques and stained with DAPI (cell nuclei), CD68 (macrophages) and PEG (LN-PLP coating). In patients treated with LN-PLP, we observed a high degree of co-localization between PEG and macrophages (Figure 1A). We observed that 88% of DAPI positive cells isolated from plaques stained positive for the macrophage marker CD68, of which 77% was also positive for liposomal PEG. As expected, CD68 positive macrophages isolated from patients treated with saline did not stain positive for PEG (Figure 1B). This finding supports the feasibility of drug delivery to plaque macrophages in patients with atherosclerotic disease.

TABLE 2. Clinical characteristics of patients in the nanomedicine delivery study

Clinical characteristic	LN-PLP (n = 7)	Placebo (n = 7)
Age	67 ± 5.9	73 ± 7.8
Gender, male n (%)	7 (100%)	6 (86%)
BMI, kg/m ²	27.3 ± 5.0	26.0 ± 5.2
SBP, mmHg	130 ± 8.0	136 ± 10.0
Lipid profile:		
TChol, mmol/L	4.4 ± 1.1	4.0 ± 1.0
LDL-c, mmol/L	2.3 ± 0.6	2.1 ± 0.5
HDL-c, mmol/L	1.1 ± 0.4	1.2 ± 0.4
TG, mmol/L	2.0 ± 1.1	2.1 ± 1.0

Data are shown as mean ± SD or number (%). BMI indicates body mass index; HDL-c, high density lipid cholesterol; LDL-c, low density lipid cholesterol; LN-PLP, liposomal prednisolone; SBP, systolic blood pressure; TChol, total cholesterol; TG, triglycerides.

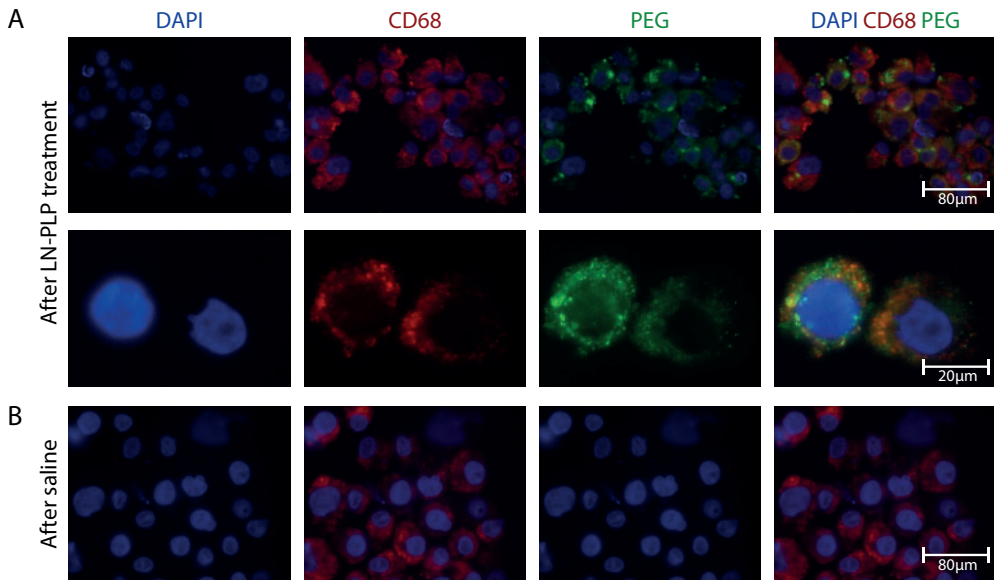


FIGURE 1. Local accumulation of LN-PLP in macrophages of iliofemoral plaques

(A) Microscopic images of cells isolated from a plaque of a patient treated with LN-PLP stained for cell nuclei (DAPI) and macrophages (CD68) and the liposome-coating PEG. Below, the enlargement of two cells corroborates the co-localization of CD68 cells and PEG. (B) Microscopic images illustrating that CD68 positive cells isolated from a plaque of a patient treated with saline do not show positivity for PEG. LN-PLP indicates liposomal prednisolone, PEG, polyethylene glycol.

LN-PLP efficacy in patients with atherosclerosis

Having established feasibility, our next step was to evaluate LN-PLP's therapeutic efficacy in patients with atherosclerotic disease. At baseline, the LN-PLP and saline treatment groups had similar clinical characteristics with the exception of higher systolic blood pressure in the saline group (Table 3). After two infusions of either LN-PLP (1.5 mg/kg) or saline, local efficacy was assessed with DCE-MRI and ^{18}F -FDG PET/CT. In contrast to the preclinical efficacy data⁹, we did not observe a reduction in arterial wall permeability after LN-PLP treatment (Table 4). Illustrative pre- and post-treatment DCE-MRI overlay images are shown in Figure 2A and 2B. The non-model-based AUC remained unaltered after two LN-PLP infusions (for the left carotid artery, 0.1143 ± 0.0619 at baseline and 0.1294 ± 0.0686 after treatment, $p=0.45$). Accordingly, the kinetic parameter K^{trans} was not reduced by LN-PLP (for the left carotid artery, 0.1062 ± 0.0659 at baseline and 0.1259 ± 0.0651 after treatment, $p=0.23$). The lack of change in AUC and K^{trans} was also observed in the right carotid artery (Table 4). Figures 2 C-F illustrate the DCE-MRI parameters for the left and right carotid arteries in both the LN-PLP and saline groups.

TABLE 3. Clinical characteristics in the efficacy study

	LN-PLP (n = 20)	Placebo (n = 10)
Inclusion parameters		
TBR _{max} AA	2.80 ± 0.42	2.81 ± 0.42
TBR _{max} LCA	1.78 ± 0.31	1.83 ± 0.24
TBR _{max} RCA	1.87 ± 0.28	1.97 ± 0.22
Baseline characteristics		
Age	61 ± 7	59 ± 7
Gender, m (m %)	16 (80%)	8 (80%)
BMI, kg/m ²	29.0 ± 4.5	28.4 ± 3.5
SBP, mmHg	130 ± 13 *	150 ± 13 *
Lipid profile		
Total cholesterol, mmol/L	5.86 ± 2.30	5.63 ± 1.71
LDL-c, mmol/L	3.96 ± 2.31	3.92 ± 1.53
HDL-c, mmol/L	1.33 ± 0.50	1.09 ± 0.45
TG, mmol/L	1.51 ± 1.10	1.56 ± 0.81

Data are shown as mean ± SD or number (%). * p<0.05. AA indicates ascending aorta; BMI, body mass index; HDL-c, high density lipid cholesterol; LCA, left carotid artery; LDL-c, low density lipid cholesterol; LN-PLP, liposomal prednisolone; RCA, right carotid artery; SBP, systolic blood pressure; TG, triglycerides.

In addition, we saw no reduction in arterial wall inflammation after LN-PLP treatment (Table 4). Figure 3A and 3B provide representative pre- and post-treatment CT and PET/CT images of a patient treated with LN-PLP. Treatment with LN-PLP resulted in a marginal 7% TBR_{max} increase in the left carotid artery (from 1.78 ± 0.31 at baseline to 1.90 ± 0.38 after treatment, p=0.03) versus no change in patients treated with placebo (from 1.82 ± 0.16 at baseline to 1.82 ± 0.24 after treatment, p=0.16; Figure 3C). Similarly, the TBR_{mean} increased 5% after LN-PLP infusions, whereas no change was observed in the saline treatment group (Figure 3E). The right carotid artery demonstrated corresponding measurements, as illustrated in Figures 3D and F. Patients tolerated LN-PLP well, with no observed changes in vital signs or lipid, inflammatory or safety markers (Table S2).

TABLE 4. DCE-MRI and PET/CT imaging at baseline and after treatment

		LN-PLP (n=20)			Placebo (n=10)		
		Pre	Post	P-value	Pre	Post	P-value
DCE-MRI							
Left carotid	AUC	0.1143±0.0619	0.1294 ± 0.0686	0.45	0.1103 ± 0.0472	0.1095 ± 0.0633	0.48
	K ^{trans}	0.1062 ± 0.0659	0.1259 ± 0.0651	0.23	0.0904 ± 0.0323	0.1005 ± 0.0475	0.25
Right carotid	AUC	0.1061 ± 0.0712	0.1195 ± 0.0732	0.48	0.0821 ± 0.0455	0.0760 ± 0.0360	0.89
	K ^{trans}	0.0929 ± 0.0673	0.1058 ± 0.0542	0.09	0.0798 ± 0.0613	0.0646 ± 0.0255	0.55
PET/CT							
Left carotid	TBR _{max}	1.78 ± 0.31	1.90± 0.38	0.03	1.82 ± 0.16	1.82 ± 0.24	0.16
	TBR _{mean}	1.43 ± 0.23	1.54± 0.29	0.01	1.42 ± 0.16	1.38 ± 0.14	0.39
Right carotid	TBR _{max}	1.87 ± 0.28	1.96± 0.38	0.05	1.86 ± 0.22	1.85 ± 0.20	0.07
	TBR _{mean}	1.51 ± 0.20	1.58± 0.26	0.04	1.57 ± 0.15	1.56 ± 0.17	0.86

Data are shown as mean ± SD. AUC, indicates area under the curve; DCE-MRI, dynamic contrast enhanced-magnetic resonance imaging; LCA, left carotid artery; LN-PLP, liposomal prednisolone; PET/CT, positron emission tomography with computer tomography; RCA, right carotid artery; TBR, target to background ratio.

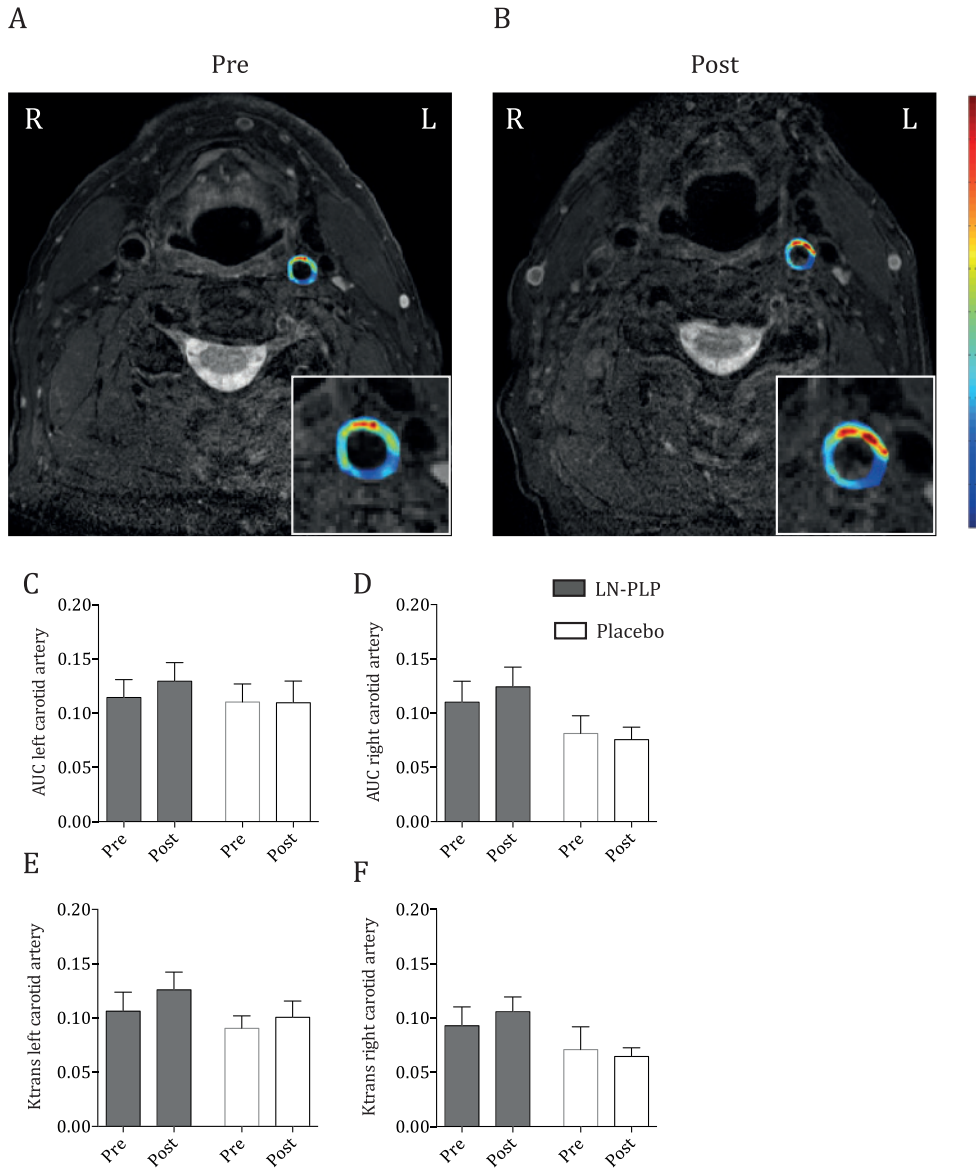


FIGURE 2. Arterial wall permeability after LN-PLP infusion in patients

(A,B) Representative axial T1-weighted MR images of the carotid arteries, the inset shows a magnification of the left carotid artery with a superimposed AUC map before and after LN-PLP treatment. (C-F) Bar graphs demonstrating the lack of reduction in AUC and K^{trans} for the left carotid artery (C,D) and right carotid artery (E,F) after LN-PLP (grey bars), compared with placebo (white bars). AUC, indicates area under the curve; LN-PLP, liposomal prednisolone; MRI, magnetic resonance imaging.

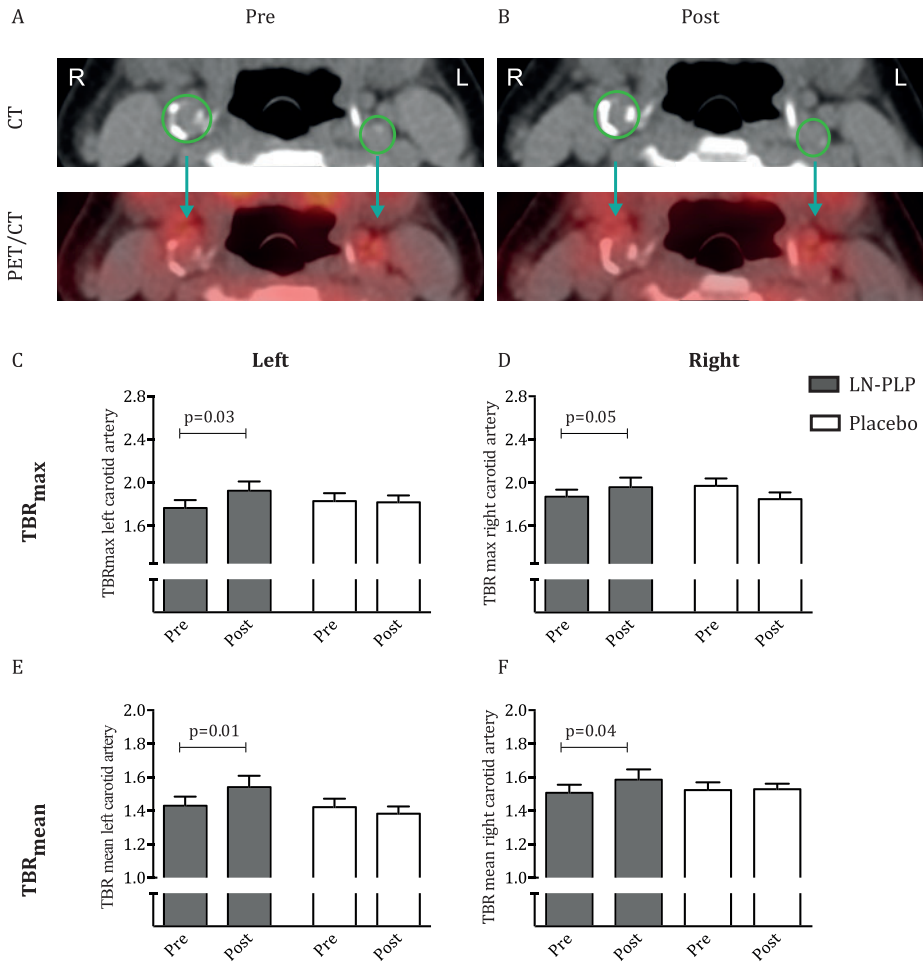


FIGURE 3. Arterial wall inflammation after LN-PLP infusion in patients

(A,B) Representative axial CT and PET/CT images of the carotid arteries before and after LN-PLP treatment, with region of interest shown in green. (C-F) Bar graphs showing the change in TBR_{max} and TBR_{mean} in the left carotid artery (C,D) and right carotid artery (E,F) after LN-PLP treatment (grey bars) or placebo (white bars). CT indicates computed tomography; LN-PLP, liposomal prednisolone; PET, positron emission tomography; TBR, target to background ratio.

DISCUSSION

Our present study aimed at exploring a liposomal nanoparticle loaded with prednisolone phosphate in the clinical frontier of atherosclerotic disease. First, we show the prolonged circulation half-life of prednisolone administered as a liposomal nanoparticle in humans, making this delivery approach potentially suitable for local delivery to atherosclerotic lesions. Indeed, we observed intravenously administered liposomal prednisolone to successfully

accumulate in macrophages isolated from atherosclerotic plaques of patients with symptomatic iliofemoral atherosclerosis. However, in atherosclerotic patients short-term LN-PLP treatment did not reduce arterial wall permeability or arterial wall inflammation, as assessed with multimodal imaging. Despite the lack of anti-inflammatory efficacy, these data show, for the first time, that nanomedicinal delivery of drugs to atherosclerotic lesions is feasible in humans.

Although its applications have been explored primarily in oncology, nanomedicine is a promising therapeutic approach to cardiovascular disease⁵. Efficient delivery to atherosclerotic lesions requires preventing rapid nanoparticle removal from plasma, predominantly by the MPS. To block nanoparticle removal and allow nanoparticles to arrive at and accumulate in plaque, hydrophilic polymers, including PEG, are usually added to nanoparticle surfaces³. In the present study, packaging prednisolone phosphate in PEG-ylated liposomes markedly prolonged the drug's half-life to 45-63 hours in humans, which is 7 to 15-fold longer than for intravenously-administrated free prednisolone phosphate⁶. These PK features will theoretically facilitate LN-PLP delivery to atherosclerotic plaques.

Intravenously infusing LN-PLP into the antecubital vein 10 and 3 days prior to iliofemoral endarterectomy led to LN-PLP accumulation in plaque macrophages taken from patients with symptomatic iliofemoral atherosclerosis. LN accumulate in plaque macrophages through two possible routes. First, nanoparticles can potentially be taken up by splenic or circulating monocytes that subsequently migrate to the plaque. However, the PEG coating is designed to serve as a steric barrier that minimizes nanoparticle opsonization and uptake by phagocytic cells¹², thus suggesting little monocyte LN uptake. Nonetheless, if circulating LN may associate with circulating or splenic monocytes, they eventually migrate to areas of inflammation through a natural conduit¹³, as has been demonstrated in mouse models of myocardial infarction and stroke¹⁴. Second, LN may extravasate due to atherosclerotic plaques' enhanced permeability, since the endothelial lining covering the atherosclerotic lesion is largely dysfunctional¹⁵. In addition, plaque's hypoxia-induced expansion of the vaso vasorum results in leaky neovessels with poor endothelial cell junctions^{16,17}. This type of increased microvessel permeability has been shown to enhance local extravasation of long-circulating nanoparticles in cancer¹⁸. Thus, the increased permeability at the luminal and/or adventitial side allows for long-circulating nanoparticles to extravasate, resulting in accumulation of the LN within the subendothelial space and eventually phagocytosis by plaque macrophages. A limitation of the trial design is that we show accumulation in the iliofemoral segment but not in other atherosclerotic areas, such as the carotid arteries. This was dictated by the availability of and access to human material of patients that were allowed to enroll by the IRB. Future human studies using non-invasively traceable LN could provide more quantitative insight in LN accumulation in different anatomical locations.

Whereas previously LN-PLP showed to reduce inflammation in atherosclerotic lesions in rabbits⁹, LN-PLP treatment did not induce measurable anti-inflammatory effects in the atherosclerotic artery wall in patients. The discrepancy in therapeutic efficacy between the preclinical rabbit

study and human trial may have several explanations.

First, it may have resulted from an insufficient dose of prednisolone reaching the plaque. Unfortunately, the present study does not allow for quantitative assessment of the concentration of prednisolone delivered to the plaque. In contrast to the previously reported 4-10% accumulation rate of intravenously infused liposomal agents in tumors¹⁹, accumulation in widely-spread plaques may not have been sufficient to exert a potent anti-inflammatory effect. While increasing the LN-PLP dose will likely resolve this issue, upping the dosage may introduce the risk of adverse effects caused by high intracellular GC concentrations. For instance, GC have been shown to polarize macrophages towards a phenotype with a higher propensity towards lipid accumulation^{20,21}, which may increase ER-stress and eventually lead to macrophage apoptosis in the plaque²². Moreover, GC-induced upregulation of 11 β -hydroxysteroid dehydrogenase type 1 (11 β -HSD1) in plaque macrophages can increase intracellular accumulation of pro-inflammatory GC^{23,24}. These inadvertent negative consequences of GC imply that, prior to increasing LN-PLP doses in patients, we should clarify intracellular GC's impact on macrophages in the lipid-rich plaque environment.

A second reason for the lack of reduced inflammation in humans may relate to a timing issue: the trial may have been too short to detect anti-inflammatory effects. Most studies evaluating the impact of anti-inflammatory agents in human cardiovascular disease showed therapeutic efficacy only after 12 weeks of treatment, whereas our study evaluated results after only 10 days, based on the rapid reduction in arterial wall inflammation following LN-PLP treatment in atherosclerotic rabbits. The fact that we observed an increase in arterial wall ¹⁸F-FDG uptake in patients, however, favors other factors than time contributing to the discrepant findings between rabbits and patients. In this respect, the pathobiology of rabbit and human atherosclerosis has marked differences. Atherosclerotic lesions in rabbits are induced in weeks following an acute injury response, whereas patients develop atherosclerotic plaques over the course of many decades. As a consequence, human atherosclerosis is characterized by complex plaques with a high lipid burden and a chronic low-grade inflammatory response. The observed differential therapeutic result between experimental and clinical atherosclerosis in the present study implies that the responsiveness of an acute injury reaction in the atherosclerotic rabbit model may not translate to anti-inflammatory compounds' efficacy in patients with advanced atherosclerosis.

Finally, the liposomal carrier may have had an adverse effect independent of the compound present inside the carrier, thereby masking a potential beneficial result. This scenario seems less likely, since the LN used in our study are composed of saturated phospholipids that are inherently resistant to oxidation or pro-inflammatory effects²⁵⁻²⁸. In accordance with our outcomes, other phase II/III studies using PEG-ylated compounds in humans have not reported pro-inflammatory effects²⁷⁻²⁹. Indeed, it has been suggested that empty liposomes can regress atherosclerosis, since such particles can act as high-capacity, low-affinity acceptors of intracellular cholesterol^{30,31}.

Nanomedicine-based delivery represents a new paradigm in the treatment of atherosclerotic disease^{5,32}. In a first-in-human anti-atherosclerosis nanotherapy trial we demonstrated that long-circulating liposomal nanoparticles accumulate in plaque macrophages of patients. This phenomenon likely also holds true for other long-circulating nanoparticle platforms, such as micellar³³ or polymeric nanoparticles³⁴. Future efforts should be aimed at the non-invasive and quantitative assessment of nanoparticle plaque targeting by imaging. This will also enable studying cardiovascular patients' heterogeneity in plaque permeability, and consequently the ability of nanoparticles to accumulate in plaques. Existing experience in rheumatoid arthritis patients with the current LN-PLP nanotherapy allowed us to accelerate its translation into cardiovascular disease. However, the GC drug payload may not have been ideal for atherosclerotic disease. Therefore, to further develop cardiovascular nanomedicine, an important focus should be on identifying suitable drug candidates for targeted treatment of human atherosclerotic plaques with a complex inflammatory, lipid-rich micro milieu.

In conclusion, we present evidence of local delivery of intravenously administered LN-PLP into macrophages isolated from human atherosclerotic plaques. In patients with atherosclerosis, however, short-term LN-PLP administration did not achieve a significant anti-inflammatory effect in atherosclerotic lesions. Nonetheless, we emphasize the potential of nanomedicine as a novel treatment paradigm for patients with atherosclerotic disease. Our work may serve as a guide for both the development as well as efficacy readout of future anti-atherosclerotic nanotherapies using imaging-assisted efficacy measures in relatively small-scaled studies.

Disclosures and funding: This work was supported by a European Framework Program 7 grant (ESS, GS: FP7-Health 309820: Nano-Athero); the Dutch network for Nanotechnology NanoNext NL, in the subprogram "Drug Delivery"; the National Heart, Lung, and Blood Institute, National Institutes of Health, as a Program of Excellence in Nanotechnology (PEN) Award, Contract #HHSN268201000045C (Z.A.F.); and NIH grants R01 HL118440 (W.J.M.M.), R01 HL125703 (W.J.M.M.), R01 EB009638 (Z.A.F.), and NWOVidi 91713324 (W.J.M.M.). Additionally, this work was supported by a grant from Enceladus Pharmaceuticals (Amsterdam, The Netherlands). M.E.L. was partially supported by the International Atherosclerosis Society (USA) and by the Foundation "De Drie Lichten" (The Netherlands). J.M.M. is affiliated with the company Enceladus Pharmaceuticals (Amsterdam, The Netherlands), and G.S. is an advisor for the company Enceladus Pharmaceuticals (Amsterdam, The Netherlands). These other authors declare that they have no competing interests. All other authors declare that they have no conflict of interest and no relationships with industry relevant to this study.

REFERENCES

1. Libby P et al. Progress and challenges in translating the biology of atherosclerosis. *Nature* 2011;473;317–25.
2. Van der Valk FM et al. Novel anti-inflammatory strategies in atherosclerosis. *Curr Opin Lipidol* 2012;23;532–9.
3. Wagner, V et al. The emerging nanomedicine landscape. *Nat Biotechnol* 2006;24;1211–7.
4. Zhang L et al. Nanoparticles in Medicine: Therapeutic Applications and Developments. *Transl Med* 2008;83;761–769.
5. Lobatto ME et al. Perspectives and opportunities for nanomedicine in the management of atherosclerosis. *Nat Rev Drug Discov* 2011;10;835–52.
6. Czock D et al. Pharmacokinetics and pharmacodynamics of systemically administered glucocorticoids. *Clin Pharmacokinet* 2005;44;61–98.
7. Wei L. Taking Glucocorticoids by Prescription Is Associated with Subsequent Cardiovascular Disease. *Ann Intern Med* 2004;141;764.
8. Wang L et al. Stent-mediated methylprednisolone delivery reduces macrophage contents and in-stent neointimal formation. *Coron Artery Dis* 2005;16;237–43.
9. Lobatto ME et al. Multimodal Clinical Imaging To Longitudinally Assess a Nanomedical Anti-Inflammatory Treatment in Experimental Atherosclerosis. *Mol Pharm* 2010;7;2020–2029.
10. Reagan-Shaw S et al. Dose translation from animal to human studies revisited. *FASEB J* 2008;22;659–61.
11. Allen TM and Cullis PR. Drug delivery systems: entering the mainstream. *Science* 2004;303;1818–22.
12. Hak S et al. The effect of nanoparticle polyethylene glycol surface density on ligand-directed tumor targeting studied in vivo by dual modality imaging. *ACS Nano* 2012;6;5648–58.
13. Swirski FK and Nahrendorf M. Leukocyte behavior in atherosclerosis, myocardial infarction, and heart failure. *Science* 2013;339;161–6.
14. Flögel U et al. In vivo monitoring of inflammation after cardiac and cerebral ischemia by fluorine magnetic resonance imaging. *Circulation* 2008;118;140–8.
15. Davignon J and Ganz P. Role of endothelial dysfunction in atherosclerosis. *Circulation* 2004;109;II27–32.
16. Virmani R et al. Atherosclerotic plaque progression and vulnerability to rupture: angiogenesis as a source of intraplaque hemorrhage. *Arterioscler Thromb Vasc Biol* 2005;25;2054–61.
17. Ritman EL and Lerman A. The dynamic vasa vasorum. *Cardiovasc Res* 2007;75;649–58.
18. Lammers T et al. Drug targeting to tumors: principles, pitfalls and (pre-) clinical progress. *J Control Release* 2012;161;175–87.
19. Bartlett D et al. Impact of tumor-specific targeting on the biodistribution and efficacy of siRNA nanoparticles measured by multimodality in vivo imaging. *Proc Natl Acad Sci U S A* 2007;104;15549–54.
20. Liew YY et al. Effect of rapamycin and prednisolone in differentiated THP-1 and U937 cells. *Transplant Proc* 2002;34;2872–3.
21. Hu W et al. Statins synergize dexamethasone-induced adipocyte fatty acid binding protein expression in macrophages. *Atherosclerosis* 2012;222;434–43.
22. Spann NJ et al. Regulated accumulation of desmosterol integrates macrophage lipid metabolism and inflammatory responses. *Cell* 2012;151;138–52.
23. Luo MJ et al. 11 β -HSD1 inhibition reduces atherosclerosis in mice by altering pro-inflammatory gene expression in the vasculature. *Physiol Genomics* 2012;7;47:57.
24. Hadoke PWF et al. Modulation of 11 β -hydroxysteroid dehydrogenase as a strategy to reduce vascular inflammation. *Curr Atheroscler Rep* 2013;15;320.
25. Alipour M et al. Safety and pharmacokinetic studies of liposomal antioxidant formulations containing N-acetylcysteine, α -tocopherol or γ -tocopherol in beagle dogs. *Toxicol Mech Methods* 2013;23;419–31.
26. Mamidi RN et al. Pharmacokinetics, efficacy and toxicity of different pegylated liposomal doxorubicin formulations in preclinical models. *Cancer Chemother Pharmacol* 2010;66;1173–84.
27. Musacchio T and Torchilin VP. Recent developments in lipid-based pharmaceutical nanocarriers. *Front Biosc* 2011;16;1388–412.

28. Torchilin VP. Recent advances with liposomes as pharmaceutical carriers. *Nat Rev Drug Discov* 2005;4:145–60.
29. Metselaar JM et al. Liposomal targeting of glucocorticoids to synovial lining cells strongly increases therapeutic benefit in collagen type II arthritis. *Ann Rheum Dis* 2004;63:348–353.
30. Dass CR and Jessup W. Apolipoprotein A-I, Cyclodextrins and Liposomes as Potential Drugs for the Reversal of Atherosclerosis. A Review. *J Pharm Pharmacol* 2000;52:731–761.
31. Rodriguez WW et al. Cholesterol mobilization and regression of atheroma in cholesterol-fed rabbits induced by large unilamellar vesicles. *Biochim Biophys Acta - Biomembr* 1998;1368:306–320.
32. Mulder WJM et al. Imaging and nanomedicine in inflammatory atherosclerosis. *Sci Transl Med* 2014;6:239.
33. Torchilin VP. Micellar nanocarriers: pharmaceutical perspectives. *Pharm Res* 2007;24:1–16.
34. Pridgen EM et al. Biodegradable, polymeric nanoparticle delivery systems for cancer therapy. *Nanomedicine* 2007;2:669–80.

SUPPLEMENT

Formulation of liposomal prednisolone. The liposomal prednisolone formulation comprises the lipids dipalmitoyl phosphatidyl choline (DPPC), cholesterol and PEG 2000 distearoyl phosphatidylethanolamine (PEG-DSPE) in a molar ratio of 62%, 33% and 5%, respectively. Water-soluble PLP was encapsulated in the aqueous interior of the LN at a starting concentration of 100 mg/mL. In order to produce 1 liter of LN-PLP under GMP conditions, 62.5 g PLP was dissolved in 450 mL of sterile water for injection. The lipid components (45.0 g DPPC, 13.4 g PEG-DSPE and 12.6 g cholesterol) were dissolved in 50 mL ethanol by heating to 70°C and continuously stirring. Subsequently, the alcoholic lipid solution was injected into the aqueous prednisolone phosphate solution to create a coarse lipid dispersion. Downsizing towards the desired particle diameter occurred by high-shear homogenization. Sterilization was achieved by continuously circulating 500 mL 1 M sodium hydroxide and rinsing with phosphate buffered water for injections until pH 7.4. To clear the formulation from free PLP and ethanol, the liposome dispersion was filtered using polysulfonate membrane capsules with a cutoff of 100 kD. A sterile phosphate buffered (pH 7.6) sucrose solution (10%) was added to compensate for the loss of filtrate from the unit. After the exchange of approximately 15 L of sucrose solution, the dispersion was shown to be devoid of free PLP (< 5% of to the encapsulated quantity). Finally, the liposome dispersion was filtered using a 0.2 µm filter unit connected to a membrane pump. Characterization assays were performed to determine particle size, polydispersity, surface charge, sterility and endotoxin content, among other features. In brief, the particle size averaged 100 nm ± 10 nm, the polydispersity index was 0.04, the ζ-potential of our liposomal particle was -2.7 ± 1.2 mV, sterility was compliant and endotoxin testing was ≤ 1.8 EU/ml. Shelf life stability studies indicate that LN-PLP remains stable in storage for at least 2 years when kept between 2 and 8 degrees C.

Macrophage isolation and staining. Plaque tissue macrophages were isolated according to the methods described by Liu et al¹⁰. In brief, fresh plaques were washed, cut into small segments of approximately 1 mm³, and incubated in a proteolytic solution containing 25 mg collagenase (Sigma, C2139, St. Louis, MO, USA), 25 mg trypsin inhibitor (Sigma, T6522, St. Louis, MO, USA) and 125 mg HEPES in 25 ml HBSS solution for 2 hours at 37 °C. Free cells were collected every 5 minutes and kept in FBS. Using a lymph-prep (d=1.077 g/ml) centrifugation gradient, macrophages were isolated and suspended in PBS + 0.2% BSA.

(DCE-)MR imaging. DCE-MRI was performed according to previously published methods¹¹. In brief, the change of signal intensity in a region of interest (ROI) during contrast agent injection was studied with a custom-made Matlab (The MathWorks, Inc., Natick, MA, USA) program. Contours were traced manually for AUC calculation. A modified Tofts model was used to calculate the exchange of contrast agent from the plasma to the tissue compartment

(K^{trans}). Quantitative MR image analysis was performed using semi-automated measurement software (VesselMass, Leiden, the Netherlands).

FDG-PET/CT imaging. FDG-PET/CT scans were performed on a Gemini time-of-flight multi-detector helical PET/CT scanner (4 min/bed position) (Philips, Best, The Netherlands) according to methods described previously¹². In brief, after 90 minutes of circulation using 200 MBq of FDG (5.5 mCi), subjects underwent PET/CT imaging initiated with a non-contrast CT for attenuation correction and anatomic co-registration. For every arterial segment (ascending aorta, left and right carotid artery) at least 5 ROIs were drawn to delineate the arterial wall. Each arterial ROI provides a mean and maximum SUV. To correct for blood pool activity in the aorta and carotids, at least 5 ROIs were placed in either the superior vena cava or jugular vein. The TBR was calculated by the ratio of mean arterial SUV mean or maximum compared with venous background activity (SUV mean). For efficacy analysis, TBR of the carotid segments were used.

TABLE S1. Safety parameters in PK study in humans

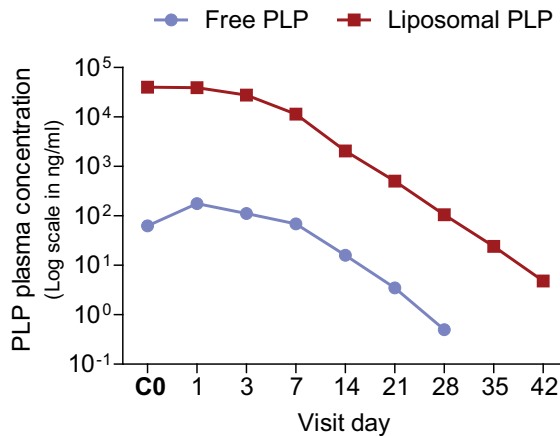
Parameter	Baseline	Week 4	Week 8	Week 12
Glucose, mmol/L	6.0 ± 2.3	5.6 ± 1.1	5.4 ± 1.3	5.6 ± 1.8
Insulin, IU/L	16.9 ± 14.4	12.7 ± 5.9	10.1 ± 3.8	11.4 ± 4.3
Cholesterol, mmol/L	5.5 ± 0.9	5.4 ± 1.0	5.2 ± 1.4	5.2 ± 1.1
LCL-c, mmol/L	3.6 ± 0.7	3.6 ± 0.9	3.5 ± 1.2	3.5 ± 0.9
HDL-c, mmol/L	1.2 ± 0.3	1.2 ± 0.3	1.2 ± 0.3	1.2 ± 0.2
Osteocalcin, µg/L	8.2 ± 2.8	na	na	8.8 ± 5.6
AP, U/L	84.8 ± 29.1	83.7 ± 20.1	82.4 ± 28.1	79.6 ± 27.9
ALT, U/L	32.6 ± 12.4	36.1 ± 13.4	28.3 ± 10.6	36.7 ± 12.8
AST, U/L	24.4 ± 8.1	23.3 ± 8.0	22.3 ± 7.7	30.1 ± 10.7
Creatinine, µmol/L	72.1 ± 15.7	77.1 ± 13.5	79.4 ± 23.7	70.4 ± 18.4

Data are shown as mean ± SD for subjects (n=8) infused intravenously with a single dose of 150mg LN-PLP. AP indicates alkaline phosphatase; ALT, alanine transaminase; AST, aspartate transaminase; HDL-c, high density lipid cholesterol; LDL-c, low density lipid cholesterol; LN-PLP, liposomal prednisolone; na, not assessed; PK, pharmacokinetic.

TABLE S2. Safety analyses of LN-PLP

Vital signs	LN-PLP (n = 20)		Placebo (n = 10)	
	Baseline	After LN-PLP	Baseline	After Placebo
SBP, mm Hg	131 ± 13	134 ± 15	150 ± 13	146 ± 11
DBP, mm Hg	80 ± 6	82 ± 10	91 ± 6	89 ± 4
Pulse, beats/min	65 ± 8	62 ± 9	71 ± 8	62 ± 10
Body temperature, °C	36.7 ± 0.5	36.6 ± 0.51	36.8 ± 0.55	36.5 ± 0.6
Body weight, kg	92 ± 18.3	91 ± 18.4	89 ± 12.2	90 ± 11.9
Safety lab				
ALT, U/L	34 ± 14	34 ± 17	35 ± 12	36 ± 10
AST, U/L	29 ± 8	23 ± 6	31 ± 4	31 ± 5
GGT, IU/L	48 ± 38	45 ± 31	30 ± 13	33 ± 15
Creatinine, µmol/L	83 ± 12	82 ± 12	77 ± 9	78 ± 10
Leukocytes, 10 ⁹ /L	5.64 ± 1.74	4.80 ± 1.22	5.33 ± 0.61	5.03 ± 0.66
Monocytes, 10 ⁹ /L	0.41 ± 0.09	0.40 ± 0.05	0.44 ± 0.13	0.46 ± 0.12
CRP, mg/L	1.82 ± 2.55	1.81 ± 1.70	2.27 ± 1.90	1.68 ± 1.53
TChol, mmol/L	5.99 ± 2.31	6.02 ± 2.37	5.62 ± 1.67	5.97 ± 1.84
LDL-c, mmol/L	4.11 ± 2.24	3.96 ± 2.16	3.92 ± 1.49	4.31 ± 1.53
HDL-c, mmol/L	1.34 ± 0.51	1.35 ± 0.52	1.09 ± 0.43	1.12 ± 0.48
TG, mmol/L	1.49 ± 1.07	1.75 ± 2.05	1.56 ± 0.76	1.66 ± 0.76

Data are shown as mean ± SD. ALT, alanine aminotransferase; AST, aspartate aminotransferase; CRP, C-reactive protein; DBP, diastolic blood pressure; GGT, gamma glutamyltransferase; HDL-c, high density lipid cholesterol; LDL-c, low density lipid cholesterol; LN-PLP, liposomal prednisolone; SBP, systolic blood pressure; TChol, total cholesterol; TG, triglycerides.

**FIGURE S1.** PK profile in humans

Line graphs showing the PLP/liposomal PLP ratio after 1.5mg/kg LN-PLP infusion, indicating that the peak plasma concentration of the free drug prednisolone (blue line) was on average 0.5% of the total liposomal PLP plasma concentration (red line), consistent throughout 28 days. LN indicates liposomal nanoparticles; PLP, prednisolone phosphate.